Sensitivity of long-wave infrared intracavity laser absorption vapor detector

Gautam Medhi[1], Chris J. Fredricksen[1], Robert E. Peale[1,*], Andrey V. Muravjov[2], Oliver J. Edwards[2]
[1]Department of Physics, University of Central Florida, Orlando, Florida, 32816 USA
[2]Zyberwear Inc., 2650 Florence Street, Orlando, Florida, 32818 USA
[*]Corresponding author: robert.peale@mail.ucf.edu

ABSTRACT

A quantum cascade laser at IR wavelengths with an open external cavity presents an opportunity for spectral sensing of molecular compounds that have low vapor pressure. The sensitivity of such a system is potentially very high due to extraordinarily long effective optical paths that can be achieved in an active cavity. We demonstrate here an external cavity mid-IR QCL molecular absorption sensor using a fixed Fabry-Perot etalon as the spectrum analyzer. The system is sensitive to the water vapor present in the laboratory air with an absorption coefficient of just 1 x 10^{-7} cm^{-1}. The system has sufficient sensitivity to detect the TNT vapor at room temperature.

Keywords: Fabry-Perot, quantum cascade laser, infrared, sensor, interferometer.

1. INTRODUCTION

Intracavity Laser Absorption Spectroscopy (ICLAS) is a well-established means of detecting and identifying weak intracavity absorbers [1]. The method involves a multimode laser with an external open cavity that allows introduction of an absorbing sample. Broadband loss inside the cavity due to optical elements is compensated by the laser amplification, allowing for much longer effective path lengths than can be achieved using passive cavities [2]. This leads to enhanced sensitivity with detection of absorption coefficients as low as 10^{-10}-10^{-11} cm^{-1} [2,3]. The highest optical path achieved was established with a CW dye laser: 70000 km [4].

Since ICLAS was first conceived in 1970 [5], different gain media have been used. These include Ti:sapphire laser [2], dye lasers [6], color center lasers [7], Nd^{3+} glass laser [8], diode lasers [9], doped fiber lasers [10], and other solid state lasers. All previous demonstrations have been in the ultraviolet to near infrared wavelength range. The mid-IR molecular fingerprint region has remained largely unexplored by this technique. There is strong reason to develop a mid-IR ICLAS system, since molecules have characteristic absorption features in the 3 to 12 μm wavelength range [11]. Such a system would have broad application in defense, security, environmental monitoring, medical diagnostics, etc.

The Quantum Cascade Laser (QCL) is the most promising mid-IR sources for ICLAS [12]. Broadband emission spectra, wide tunability, high output power, high duty cycle, and room temperature operation [13] are some of the features that make QCLs attractive for applications such as spectral sensing. The molecular finger print region (3-12 μm), where fundamental rotational-vibrational transitions of most molecules lie, is fully accessible using QCLs, which provide opportunity for constructing portable hand held sensors [14]. Working at wavelengths corresponding to the vibrational fundamentals gives the highest possible absorption cross sections and improves the sensitivity over competing techniques based on detection of overtone bands at shorter wavelengths [15].

Sensing via ICLAS is enabled by operating QCLs in an open external cavity. The first external cavity QCL (EC-QCL) was demonstrated in 2001 at cryogenic temperature [16], and since then many groups [17,18,19] have implemented it. All these works have been performed using a diffraction grating as external feedback reflector, either in Littrow [20] or Littman-Metcalf [18] configuration, for the purpose of fine tuning the output spectrum over a dense quasi-continuous longitudinal mode spectrum. In contrast, here we implement a Fabry-Perot (FP) type external cavity,

where the QCL gain medium is placed between two plane mirrors. The effective achieved optical path length of several kilometers, with the laser operating simultaneously over a broad mode spectrum, allows detection of intracavity molecular absorbers with high sensitivity.

The emission spectrum of the laser in presence of an intracavity absorber is analyzed using a fixed Fabry-Perot etalon. The laser spectrum may be observed on an oscilloscope as it self-tunes through the FP pass band. With this configuration, we estimate a sensitivity to absorption coefficients as small as 1 x 10^{-7} cm^{-1}. This value is comparable to the absorption coefficient for saturated vapor of the explosive TNT at room temperature.

2. EXPERIMENT

For first vapor-detection demonstration and subsequent system optimization we selected acetone as the target vapor, since this solvent has high vapor pressure and a well-established spectrum [11]. We procured a QCL (Maxion) with 8.06 µm center wavelength to coincide with the wing of an acetone absorption band. The QCL had one end facet high-reflection (HR) coated and the other anti-reflection (AR) coated to allow establishment of an open external cavity. Fig.1 shows the schematic of the experimental setup. The QCL was placed at the focal point of a 90° off-axis gold-coated parabolic mirror of focal length 2.5 cm with its AR coated facet facing towards the parabolic mirror. The external cavity is formed by the high reflecting back facet of the QCL chip and an external flat mirror (gold coated) with an outcoupling aperture. The signal from the external cavity then passed through the FP analyzer. The FP is formed from a pair of ZnSe flats of 2 mm thickness, with high reflection coatings (97.5%) on the facing surfaces, and AR coatings on the outer surfaces. The flats were wedged (30-arcmin) to eliminate unwanted secondary FP resonances within the substrates themselves and to prevent reflections back into the cavity. The radiation transmitted by the FP was detected using a 77 K HgCdTe detector. The length of the external cavity was ~ 33 cm. Laser emission, and acetone absorption spectra were characterized using a Bomem DA8 Fourier spectrometer with globar source, KBr beamsplitter, and 77 K HgCdTe detector.

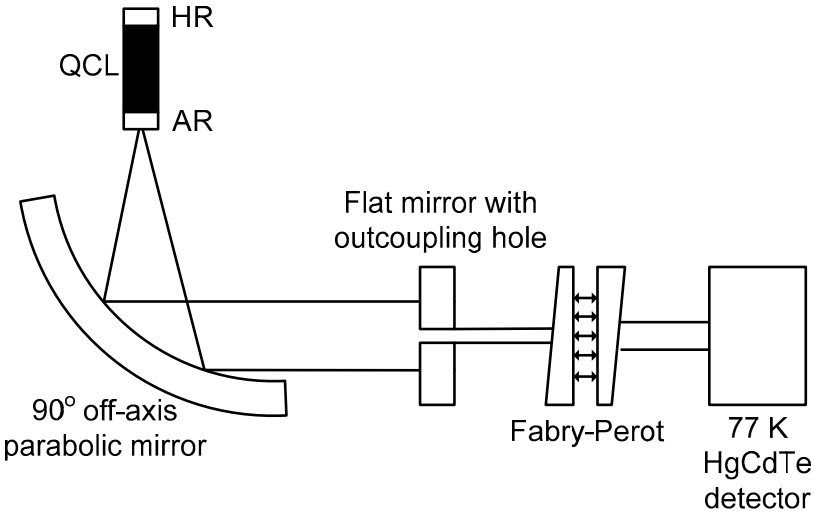

Figure 1: Schematic of the external cavity mid-IR QCL set up. The external cavity signal is analyzed by Fabry-Perot interferometer outside the cavity.

3. RESULTS

Fig. 2 compares the absorption spectrum of acetone [11] and the cw emission spectrum of the external-cavity QCL with and without a trace quantity of acetone vapor in the cavity. The acetone absorption varies monotonically across the 1230 to 1260 cm^{-1} (7.93 to 8.13 µm wavelength) gain band of the QCL. The high-resolution spectrum [21] measured at

the resolution limit of the spectrometer (0.017 cm^{-1}) reveals fine structure with individual mode separation of ~0.03 cm^{-1} due to the longitudinal modes of the external cavity [21]. The effect of the acetone vapor, which was near the limit of human olfactory detection (41 ppm [22]), is to shift the laser emission spectrum by 6 cm^{-1} toward the region of lower acetone absorption. Since the concentration of acetone introduced into the cavity was not accurately known, it is difficult to quantify the system sensitivity from this measurement. Instead, we turn our attention to the effect of humidity since the concentration of water vapor in the lab can be estimated with fair accuracy.

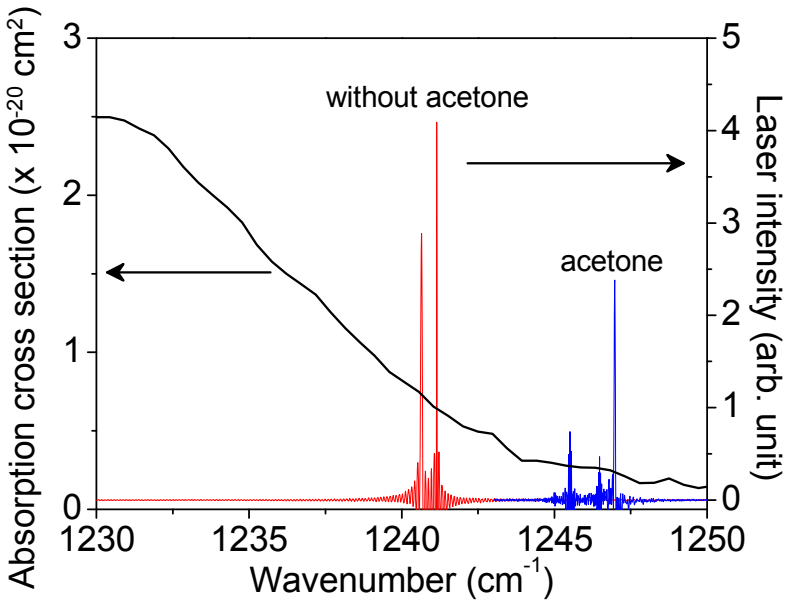

Figure 2: Absorption spectrum of acetone and QCL emission spectrum with and without trace acetone vapor inside the cavity.

Spectroscopy of the external cavity mid-IR QCL system shows that the emission spectrum stabilizes after ~1 ms of pulse duration. For shorter pulses, the spectrum is very unstable due to fast temperature rise in the active crystal, causing poor repeatability of the spectrum dynamics. After 1 ms, the spectrum stabilizes but continues a slow adiabatic drift due to the continued slow drift of the active chip temperature. This slow but stable shift of the emission spectrum is very repeatable from pulse to pulse, allowing us to monitor the mode spectrum as it passes through the narrow fixed transmission resonance of the FP. The spectrum may be observed in real time on an oscilloscope (albeit with a non-linear wavelength scale due to non-linear but monotonic temperature increase with time).

In this configuration the system is found to be sensitive to water vapor in the ambient laboratory air. Thus an accurate estimation of water vapor absorption coefficient at 8.06 μm is important for the system sensitivity estimation. Fig. 3 presents an atmospheric transmittance (T) spectrum in the 7.9-8.3 μm wavelength range [23,24]. The 8.06 μm QCL wavelength is indicated by a symbol. Since the wavelength falls at the edge of the 8-12 μm "water window", the absorption coefficient is small. The optical path length L was 300 m and the precipitable water content PWC was 5.7 mm.

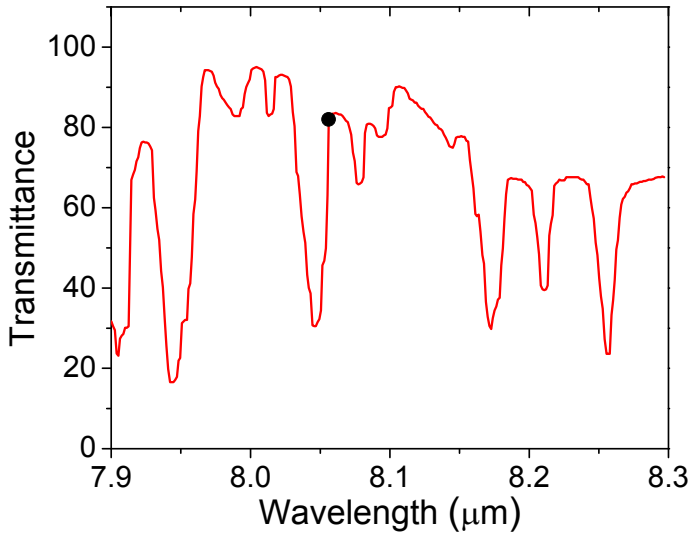

Figure 3: Atmospheric transmission spectrum, adopted from ref [22,23]. The symbol indicates the wavelength position of the QCL.

Precipitable water content (PWC) is defined as the thickness of the slab of liquid water that would be formed if all of the water vapor along the line of sight was condensed [25]. From the values of PWC and L, the number density n of water molecules in vapor is immediately determined according to

$$n = \frac{\rho\, PWC\, N_A}{L\, m}, \qquad (1)$$

where ρ is the density of liquid water, N_A Avogadro's number, and m the molar mass of water. For the condition of the Fig. 3 spectrum we find $n = 6.3 \times 10^{17}$ cm^{-3}.

From the transmittance curve in Fig. 3, we determine the absorption coefficient using the Beer-Lambert law $\alpha = -\frac{1}{L} lnT$. The determined value at the 8.06 μm is 7.0×10^{-6} cm^{-1}. The absorption cross-section, $\sigma = \frac{\alpha}{n}$, is therefore 1.1×10^{-23} cm^2.

The saturated water vapor number density (n_s) at lab temperature of 23° C is 6.45×10^{17} cm^{-3}, according to [26]. In the climate-controlled air of a laboratory (T = 23° C), RH ~ 40%, [25]. Thus the number density of water molecules in the lab is $n = RH \times n_s = 2.6 \times 10^{17}$ cm^{-3}. The corresponding absorption coefficient at the laser wavelength is 2.9×10^{-6} cm^{-1}.

Fig. 4 presents the oscilloscope traces that reveal the effect of intracavity humidity on the laser spectrum. The time axis corresponds (non-linearly) to the emission wavelength due to the thermal drift of the laser spectrum through the narrow FP pass band. The QCL wavelength is known to shift toward longer wavelength as the chip temperature increases. The QCL was excited for a pulse duration of 5 ms as shown by the square current monitor trace in Fig. 4. In the upper plot ~ 12 modes are observed passing through the transmission maximum of the fixed etalon between the start of the laser pulse at 0 ms and 2.5 ms. After 2.5 ms, the laser no longer operates within the etalon pass band. That the laser is capable of cw operation rules out the possibility that it has simply stopped emitting after 2.5 ms. Rather, the emission has simply shifted to wavelengths well removed from the etalon pass band.

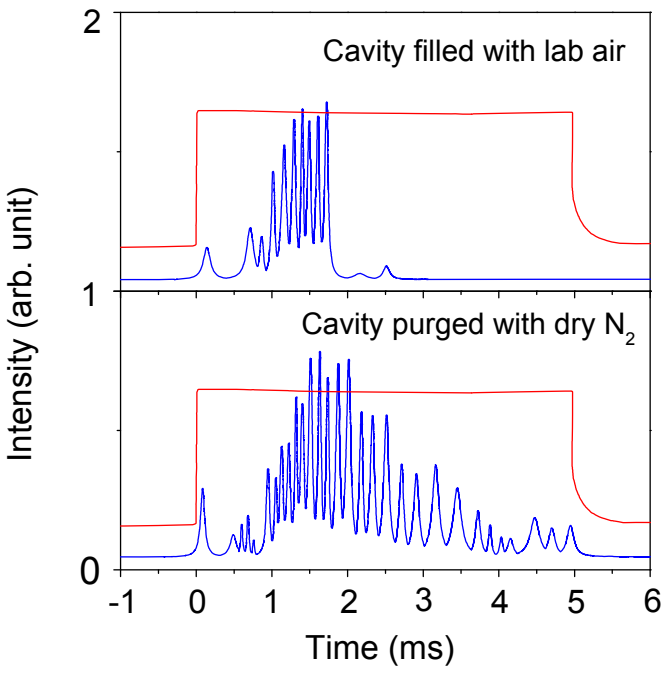

Figure 4: Oscilloscope traces of the spectral dynamics of the external cavity configuration. (top) cavity filled with lab air (bottom) cavity purged with dry nitrogen. The QCL was excited slightly above the threshold current at pulse duration of 5 ms and 20% duty cycle. The current profile in the active chip during the pulse is also shown by the square wave in each plot.

The lower plot in Fig. 4 shows that purging the cavity with dry nitrogen causes 10-12 additional modes to pass through the etalon pass band after 2.5 ms, where no modes were seen before. The laser spectrum returned to its original position when room air was reintroduced. This confirms that the system is sensitive to laboratory humidity with an absorption coefficient at the level of 2.9 x 10^{-6} cm^{-1}.

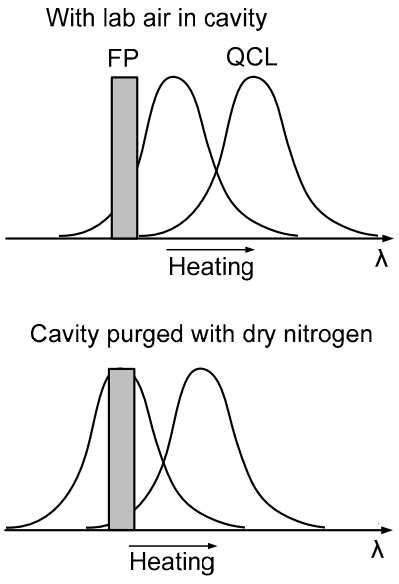

Figure 5: Schematic of shift of multimode QCL emission band due to heating by excitation pulse with respect to Fabry-Perot pass band.

Purging the cavity with dry nitrogen removes water vapor absorption from the cavity. The laser might be expected to operate at entirely new wavelength based on its response to acetone vapor (Fig. 2). If the shift due to purging is opposite to the direction of the shift due to heating, then one might expect that more of the multimode emission band may now pass through the etalon as the laser heats during the pulse. Given the position of the laser wavelength on the long wavelength shoulder of a water absorption line (Fig. 3), the emission wavelength might well be expected to shift to shorter wavelengths when water is removed from the cavity. This effect is explained schematically in Fig. 5.

The sensitivity of the system is thus defined by this demonstration. A shift in the spectrum by ~ 10 modes was observed when purging the cavity of 2.6 x 10^{17} cm^{-3} water molecules. In reality the change in the absorption coefficient due to purging with N_2 was less than the stated 2.9 x 10^{-6} cm^{-1} by as much as a factor of 3, since the cavity was inefficiently tented to affect the purge. Moreover a shift of one mode should be observable. These considerations imply an absorption coefficient change ~ 30 times less on purging, or ~ 1 x 10^{-7} cm^{-1}.

The observed system response allows an estimate of sensitivity to 2,4,6-trinitrotoluene (TNT). TNT has a vapor pressure less than 10^{-5} Torr at room temperature. We used TNT vapor absorption spectra at higher temperature [27] to calculate its absorption cross-section. TNT vapor spectra show two dominant peaks at 6.41 and 7.41 μm wavelengths, Fig. 6 inset (bottom right). The ordinate in the right hand side in Fig. 6 shows the peak absorption coefficients of TNT at these two wavelengths. As the full width half maximum (FWHM) of these two absorption lines are nearly temperature independent, the peak absorption coefficients are proportional to the cross sections of the TNT. The ordinate on the left hand side in Fig. 6 shows the vapor pressure of TNT at different elevated temperatures, calculated using Clausius-Clapeyron equation [28] with the fitting parameter given in [29]. Comparison with the absorption coefficient curve (right ordinate) confirms that the values are proportional as expected. The TNT vapor absorption cross section is then calculated from $\sigma = \frac{\alpha}{n} = \frac{\alpha kT}{P}$. For the stronger line, the peak absorption cross-sections determined from the average of the Fig. 6 data is 7.85 x 10^{-19} cm^2. The concentration of TNT at room temperature is $n = \frac{P}{kT} = 3.25 \times 10^{11}$ cm^{-3}. Thus the absorption coefficient of TNT at room temperature is $\alpha = \sigma \times n$ = 2.5 x 10^{-7} cm^{-1} at 6.41 μm wavelength. Thus the estimated system sensitivity is already within a factor of 2.5 of being able to detect the saturated vapor of TNT. This factor is probably within the uncertainty, and we believe that there is at least an order of magnitude room for system improvement.

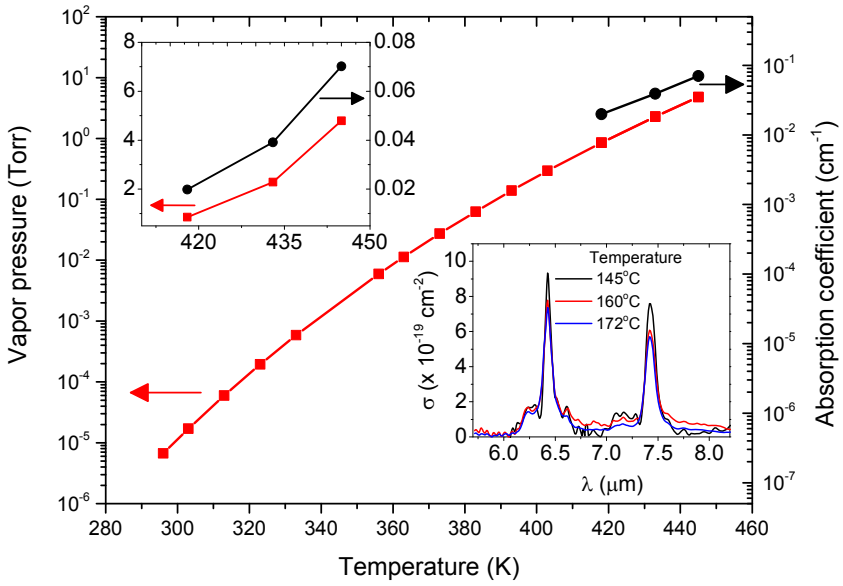

Figure 6: Peak absorption coefficient and vapor pressure of TNT measured at different elevated temperature. The insets (top left) shows the same in a linear scale at three different elevated temperatures and (bottom right) the two dominant peaks at 6.41 and 7.41 μm wavelength.

4. SUMMARY

The sensitivity to trace intracavity vapors of an external cavity mid-IR QCL at 8.06 μm is estimated when the system is combined with a fixed Fabry-Perot interferometer. The emission spectrum is highly sensitive to the presence of weak acetone or water vapor absorption in the cavity. The estimated sensitivity is 1 x 10^{-7} cm^{-1} which is about the required level to detect saturated vapors of TNT.

ACKNOWLEDGMENT

This project is supported by US Army Phase RDECOM Phase II SBIR contract W911NF-10-C-0030 to Zyberwear, Inc., under the ARO program management of Dr. Dwight Woolard.

REFERENCES

[1] Baev,V.M., Latz, T., Latz, Toschek, T.E., "Laser Intracavity absorption spectroscopy", Applied Physics B **69**, 171-202 (1999).
[2] Kachanov, A., Charvat, A., Stoeckel, F., "Intracavity laser spectroscopy with vibronic solid-state lasers: I. Spectro-temporal transient behaviour of a Ti:sapphire laser", J. Opt. Soc. Am. B **11**, 2412-2421 (1994).
[3] Garnache, A., Kachanov, A. A., Stoeckel, F., "High-sensitivity intracavity laser absorption spectroscopy with vertical-external-cavity surface-emitting semiconductor lasers", Optics Letters, **24**, 826-828 (1999).
[4] Sierks, J., Latz, T., Baev, V. M., Toschek, P. E., "Spectral dynamics of multi-mode dye lasers and single atom absorption", in Intl. Quantum Electronics Conf., OSA Technical Digest Series (Optical Society of America, Washington DC, (1996).
[5] Pakhomycheva, L. N., Sviridenkov, E. A., Suchkov, A. F., Titova, L. A., Churilov, S. S., "Line Structure of Generation Spectra of Lasers with Inhomogeneous Broadening of the Amplification Line", J. Experimental and Theoretical Physics Lett. **12**, 43-45 (1970).
[6] Hänsch, T. W., Schawlow, A. L., Toschek, P. W., "Ultrasensitive response of a cw dye laser to selective extinction", IEEE J. Quantum Electronics **QE-8**, 802-804 (1972).
[7] Baev, V. M., Schröder, H., Toschek, P. E., "LiF:F_2^+-Center Laser for Intracavity Spectroscopy", Opt. Commun. **36**, 57-62 (1981).
[8] Bykov, A. D., Lopasov, V. P., Makushkin, Yu. S., Sinitsa, L. N., Ulenikov, O. N., Zuev, V. E., "Rotation-vibration spectra of deuterated water vapor in the 9160-9390-cm^{-1} region", J. Mol. Spectrosc. **94**, 1-27 (1982).
[9] Baev, V. M., Eschner, J., Paeth, E., Schuler, R., Toschek, P. E., "Intra-cavity spectroscopy with diode lasers", Appl. Phys. B **55**, 463-477 (1992).
[10] Böhm, R., Stephani, A., Baev, V. M., Toschek, P. E., "Intracavity absorption spectroscopy with a Nd^{3+}-doped fiber laser", Opt. Lett. **18**, 1955-1957 (1993).
[11] Peale, R. E., Muravjov, A. V., Fredricksen, C. J., Boreman,G. D., "Spectral Signatures Of Acetone Vapor From Ultraviolet To Millimeter Wavelengths", Proc. Intl. Symp. Spectral Sensing Research, Bar Harbour ME June (2006).
[12] Faist, J., Capasso, F., Sivco, D. L., Sirtori, C., Hutchinson, A. L., Cho, A. Y., 'Quantum Cascade Laser', Science, 264, 553-556 (1994).
[13] Wen Qing and Michaelian, Kirk H., "Mid-infrared photoaccustic spectroscopy of solids using an external cavity quantum-cascade-laser", Optics Lett., 33, 1875-1877, (2008).
[14] Kosterev, A. A., Curl, R. F., Tittel, F. K., Rochat, M., Beck, M., Hofstetter, D., Faist, J., "Chemical sensing with pulsed QC-DFB lasers operating at 15.6 μm", Applied Physics B: Lasers and Optics 75, 351-357,(2002).
[15] Karpf Andrea and Rao, Gottipaty N., "Absorption and wavelength modulation spectroscopy of NO2 using a tunable, external cavity continuous wave quantum cascade laser", Applied Optics, 48, 408-413, (2009).
[16] Luo, G. P., Peng, C., Le, H. Q., and Pei, S. S., "Grating-tuned external-cavity quantum-cascade semiconductor lasers", Applied Physics Letters, 78, 2834-2836 (2001).
[17] Totschnig, G., Winter, F., Pustogov, V., Faist, J., and Muller, A., "Mid-infrared external-cavity quantum cascade laser", *Opt. Lett.* 27 1788–90 (2002).
[18] Luo, G. P., Peng, C., Lee, H. Q., Pei, S. S., Lee, H., Hwang, W. Y., Ishaug, B., and Zheng, J., "Broadly wavelength-tunable external cavity mid-infrared quantum cascade lasers", *IEEE J. Quantum Electron.* 38 486–94 (2002).

[19] Maulini, R., Beck, M., Faist, J., and Gini, E., "Broadband tuning of external cavity bound-to-continuum quantum-cascade lasers", *Appl. Phys. Lett.* 84 1659–61(2004).
[20] Tsai, T., Wysocki, G., "Fast wavelength tuning of external cavity quantum cascade lasers", Lasers and Electro-Optics, 2009 and 2009 Conference on Quantum electronics and Laser Science Conference. CLEO/QELS (2009).
[21] Medhi, G., Muravjov, A. V., Saxena, H., Fredricksen, C. J., Brusentsova, T., Peale, R. E., Edwards, O., "Intracavity laser absoption spectroscopy using mid-IR quantum cascade laser", Proc. SPIE 8032, 12-19 (2011).
[22] C.J. Wysocki, P. Dalton, M.J.Brody, H.J. Lawley, "Acetone odor and irritation thresholds obtained from acetone-exposed factory workers and from control (occupationally unexposed) subjects", American Industrial Hygiene Association Journal 58, 704-12 (1997).
[23] Yates, H. W., and Taylor, J. H., "Infrared transmission of the atmosphere", NRL report, U.S. Naval Research Laboratory, Washington D.C., (1960).
[24] Wolfe, W. L., [Handbook of military infrared technology], Office of Naval Research, Dept. of the Navy, 253, (1965).
[25] Hudson, Richard D., Jr, [Infrared System Engineering], John Wiley & Sons, (1969).
[26] Parish, O. Owen., and Putnam, Terrill. W., 'Equations for the determination of humidity from dewpoint and psychrometric data', NASA technical note, (1977).
[27] Medhi, G., Muraviev, A. V., Saxena, H., Cleary, J. W., Fredricksen, C. J., Peale, R. E., and Edwards, O., "Infrared intracavity laser absorption spectrometer", in Proc. Intl. Symp. Spectral Sensing Research, Springfield, Missouri June 21-24, (2010).
[28] Brusentsova, Tatiana N., Peale, R. E., Muravjov, A. V., Chen, L. P., Jack, M. D., Gritz, M. A., "Terahertz Spectroscopy of TNT for Explosive Detection", in Terahertz For Military And Security Applications V (DS07), edited by James O. Jensen and Hong-Liang Cui, Proc. SPIE 6549 (2007).
[29] Pella, P. A., "Measurement of the vapor pressure of TNT, 2,4-DNT, 2,6-DNT, and EGDN", Journal of chemical Thermodynamics, 9, 301-305, (1977).